

Periodic and localized waves in parabolic-law media with third- and fourth-order dispersionsHouria Triki¹ and Vladimir I. Kruglov² ¹*Radiation Physics Laboratory, Department of Physics, Faculty of Sciences, Badji Mokhtar University, P. O. Box 12, 23000 Annaba, Algeria*²*Centre for Engineering Quantum Systems, School of Mathematics and Physics, The University of Queensland, Brisbane, Queensland 4072, Australia*

(Received 11 April 2022; accepted 11 October 2022; published 26 October 2022)

Considering the higher-order nonlinearity is essential in a broad range of real physical media as it significantly influences the wave dynamics in these systems. We study the propagation of femtosecond light pulses inside an optical fiber medium exhibiting higher-order dispersion and cubic-quintic nonlinearities. Pulse evolution in such a system is governed by a higher-order nonlinear Schrödinger equation incorporating second-, third-, and fourth-order dispersions as well as cubic and quintic nonlinearities. The periodic and solitary wave solutions are identified using the equation method. Results presented indicated the potentially rich set of periodic waves in the system under the combined influence of higher-order dispersive effects and cubic-quintic nonlinearity. The velocity of these structures is uniquely dependent on all orders of dispersion. Conditions on the optical fiber parameters for the existence of these exact stable solutions are found by analytical stability analysis.

DOI: [10.1103/PhysRevE.106.044214](https://doi.org/10.1103/PhysRevE.106.044214)**I. INTRODUCTION**

A soliton in an optical fiber medium can form when the group velocity dispersion is exactly balanced by self-phase modulation. This localized pulse is found in two distinct types called bright and dark solitons which are existent in the anomalous and normal dispersion regimes, respectively. The unique property of optical solitons, either bright or dark, is their particlelike behavior in interaction [1]. Because of their robust nature, such wave packets have been successfully utilized as the information carriers (optical bits) to transmit digital signals over long propagation distances.

Studies of soliton formation in the femtosecond time scale is an important direction of research in nonlinear optics. This because femtosecond duration pulses are required for wide-ranging potential applications such as ultrahigh-bit-rate optical communication systems, optical sampling systems, infrared time-resolved spectroscopy, and ultrafast physical processes [2,3]. But when these ultrashort pulses are injected in a fiber medium, several higher-order nonlinear effects come into play along with dispersive effects which may significantly change the physical features and stability of optical soliton propagation. Important higher-order effects include third-order dispersion, self-steepening, and self-frequency shift which become important if light pulses are shorter than 100 fs [2]. Taking into account the influence of various processes appearing in the femtosecond regime, the description of signal propagation through an optical fiber medium can be achieved by use of the NLS family of equations incorporating additional higher-order terms. Compared with solitons in Kerr-like media, solitary waves supported by higher-order nonlinear and dispersive effects when they exist can demonstrate much richer dynamics as they propagate through the system. The contribution of these higher-order effects can also lead to the formation of novel structures in optical media,

including for example dipole solitons [4], W-shaped solitons [5], and multipole solitons [6].

It is worth pointing out that the necessity to take into account higher-order Kerr nonlinearity (see, e.g., Refs. [7,8]) involves a broad range of nonlinear phenomena in different physical media like organic materials [9], semiconductor-doped fibers [10], and metal-dielectric nanocomposites [11]. Such higher-order Kerr effect plays a key role for the understanding of filamentation [12], high-harmonic generation [13], plasma dynamics in both bulk and gases [14], and the formation of dissipative solitons [15]. Interestingly enough, the higher-order nonlinearities such as those occurring in cubic-quintic media may help to achieve stability of spatial solitons [16] and dissipative solitons [17]. Recent results on metamaterials also showed that the modulation instability gain is enhanced due to the simultaneous contributions of higher-order nonlinearities (such as cubic-quintic nonlinearity) [18]. All those pertinent studies demonstrate important results related to nonlinear phenomena arising due to the presence of higher-order Kerr nonlinearity in real physical systems.

Recently, attention has been focused on analyzing the dynamic behavior of soliton pulses in optical fibers exhibiting second-, third-, and fourth-order dispersions [19–21]. In addition to localized pulses, periodic waves play a significant role in the analysis of the data transmission in fiber-optic telecommunications links [22]. Because of their structural stability with respect to the small input profile perturbations and collisions [23], this kind of nonlinear wave serves as a model of pulse train propagation in optics fibers [22]. It is relevant to mention that the occurrence of periodic waves is not only restricted to optical fibers [24,25], but also to other physical systems such as Bose-Einstein condensates [26,27], nonlinear negative index materials [28,29], and nonlocal media [30]. The significant results have been obtained within the framework of the high dispersive cubic-quintic NLSE [31].

For example, Xie *et al.* [32] employed the complete discrimination system method to obtain distinct exact solutions to the high dispersive cubic-quintic NLSE. Furthermore, Xie and Tang [33] applied the bifurcation theory of dynamical systems and obtained exact solutions, and particularly solitary wave solutions for this model. The dark and bright solitary wave solutions for this NLSE were also obtained by Hua-Mei *et al.* [34] and Sultan *et al.* [35] have found the soliton solutions in various forms of the model. In addition, Hosseini *et al.* [36] utilized the special scheme to derive dark and periodic solitary wave solutions.

In this paper, we present different periodic and solitary waves which can be formed in an optical fiber medium exhibiting all orders of dispersion up to the fourth order as well as cubic and quintic nonlinearities. We introduced a special procedure, whereby it becomes possible to derive periodic and localized wave solutions of the envelope equation explicitly and to determine the conditions under which these structures exist. We especially note that the finding of localized waves is greatly desired as these pulses are ideal instruments for data transmission over fiber-optic communications lines. Moreover, the conditions on optical fiber parameters for the existence of these stable solutions are found by analytical stability analysis.

This paper is organized as follows. Section II presents the method used for obtaining traveling wave solutions of the higher-order NLSE that governs the propagation of femtosecond light pulses through a highly dispersive optical cubic-quintic medium. In Sec. III, we identify classes of periodic wave solutions based on an appropriate differential equation. We also find the solitary wave solutions of the model in the long wave limit and present the conditions on the optical fiber parameters for their existence. In Sec. IV, we present the analytical stability analysis of those periodic and solitary wave solutions based on the theory of optical nonlinear dispersive waves. Numerical results for the stability of the solutions are reported in Sec. V. Subsequently, in Sec. VI, we present a physical discussion and some applications of the studied theoretical model. Finally, we summarize our work in Sec. VII.

II. MODEL AND TRAVELING WAVES

Ultrashort light pulse propagation in a highly dispersive optical fiber exhibiting a parabolic nonlinearity law obeys the following high dispersive cubic-quintic NLSE [31]:

$$i \frac{\partial \psi}{\partial z} = \alpha \frac{\partial^2 \psi}{\partial \tau^2} + i\rho \frac{\partial^3 \psi}{\partial \tau^3} - v \frac{\partial^4 \psi}{\partial \tau^4} - \gamma |\psi|^2 \psi + \mu |\psi|^4 \psi, \quad (1)$$

where $\psi(z, \tau)$ is the complex field envelope, z represents the distance along direction of propagation, and $\tau = t - \beta_1 z$ is the retarded time in the frame moving with the group velocity of wave packets. Also $\alpha = \beta_2/2$, $\rho = \beta_3/6$, and $v = \beta_4/24$, with $\beta_k = (d^k \beta / d\omega^k)_{\omega=\omega_0}$, denotes the k -order dispersion of the optical fiber with $\beta(\omega)$ being the propagation constant depending on the optical frequency. Parameters γ and μ govern the effects of cubic and quintic nonlinearity, respectively.

For relatively long optical pulses having width more than 10 ps, all three parameters of third- and fourth-order dispersions and quintic nonlinearity are so small that the model (1) reduces to the standard NLSE which is completely integrable by the inverse scattering method [37]. In the absence of quintic nonlinearity ($\mu = 0$), solitonlike solution having a sech^2 shape and dipole soliton solution of Eq. (1) have been found by employing a regular method [19,20]. In practice, however, the quintic nonlinearity plays a significant role in the response of many optical materials and can therefore affect the temporal evolution of optical fields. We therefore analyze the situation in which the effect of quintic nonlinearity is important and should be taken into account along with all orders of dispersion up to the fourth order, as described by the underlying equation (1). It is worth mentioning here that the nontrivial contribution of the quintic nonlinearity has been demonstrated experimentally in many optical materials such as chalcogenide glasses [38], polydiacetylene toluene sulfonate (PTS) [39], semiconductors (e.g., $\text{Al}_x\text{Ga}_{1-x}\text{As}$, CdS , and $\text{CdS}_{1-x}\text{Se}_x$) waveguides, and semiconductor-doped glasses (see, e.g., Ref. [40]). From a theoretical standpoint, such a nonlinear process occurs from the expansion of the refractive index in powers of the light pulse intensity I as [41] $n = n_0 + n_2 I - n_4 I^2$, where n_0 is the linear refractive index coefficient and n_2 is the cubic nonlinearity coefficient which is related to third-order susceptibility as $n_2 = 3\chi^{(3)}/8n_0$, while n_4 is the quintic nonlinearity coefficient which is related to the fifth-order susceptibility as $n_4 = 5\chi^{(5)}/16n_0$. Physically, this kind of nonlinearity becomes important when the intensity of the light pulse exceeds a certain value, thus leading to a change in the features and stability of propagating waves.

In order to determine the exact traveling wave solutions of Eq. (1), we consider a solution of the form

$$\psi(z, \tau) = u(\xi) \exp[i(\kappa z - \delta \tau + \theta)], \quad (2)$$

where $u(\xi)$ is a real amplitude function which depends on the variable $\xi = \tau - qz$, with $q = v^{-1}$ being the inverse velocity. Also the real parameters κ and δ represent the wave number and frequency shift, respectively, while θ represents the phase of the pulse at $z = 0$.

From substitution of the representation (2) into Eq. (1), one finds the following system of ordinary differential equations:

$$v \frac{d^4 u}{d\xi^4} - (\alpha + 3\rho\delta + 6v\delta^2) \frac{d^2 u}{d\xi^2} + \gamma u^3 - \mu u^5 - (\kappa - \alpha\delta^2 - \rho\delta^3 - v\delta^4) u = 0, \quad (3)$$

$$(\rho + 4v\delta) \frac{d^3 u}{d\xi^3} + (q - 2\alpha\delta - 3\rho\delta^2 - 4v\delta^3) \frac{du}{d\xi} = 0. \quad (4)$$

Then from Eq. (4), we find that nontrivial solutions for Eqs. (3) and (4) with $v \neq 0$ can exist for values of the frequency shift δ and inverse velocity q satisfying the relations

$$\delta = -\frac{\rho}{4v}, \quad q = 2\alpha\delta + 3\rho\delta^2 + 4v\delta^3. \quad (5)$$

We can make use of the parameters in (5) to determine the wave velocity $v = q^{-1}$ as

$$v = \frac{8v^2}{\rho(\rho^2 - 4\alpha v)}. \tag{6}$$

Relation (6) shows that the velocity of propagating waves is uniquely dependent on the parameters of second-, third-, and fourth-order dispersions and it does not depend upon the nonlinearity parameters. Therefore, a natural way to control the velocity of a pulse is to vary various dispersion parameters in the fiber.

On further substitution of Eq. (5) into Eq. (3), we obtain an evolution equation for $u(\xi)$ as

$$\frac{d^4 u}{d\xi^4} + \lambda_0 \frac{d^2 u}{d\xi^2} + \lambda_1 u + \lambda_2 u^3 + \lambda_3 u^5 = 0, \tag{7}$$

where the parameters λ_n ($n = 0, \dots, 3$) are defined by

$$\lambda_0 = \frac{3\rho^2}{8v^2} - \frac{\alpha}{v}, \quad \lambda_1 = -\frac{\kappa}{v} - \frac{\rho^2}{16v^3} \left(\frac{3\rho^2}{16v} - \alpha \right), \tag{8}$$

$$\lambda_2 = \frac{\gamma}{v}, \quad \lambda_3 = -\frac{\mu}{v}. \tag{9}$$

It is critically important to find exact analytical localized and periodic solutions of the amplitude equation (7) in the most general case, when all parameters of Eq. (1) have nonzero values and no constraint for them. This enables us to examine the individual influence of each type of dispersive and nonlinear effect on the characteristics of propagating nonlinear waves. It is interesting to point out that the finding of such closed form solutions is greatly desired to experiments as they give a precise formulation of the existing solitary and periodic pulses.

We observe that the nonlinear differential equation (7) includes two coexisting cubic u^3 and quintic u^5 nonlinear terms in addition to two even-order derivative terms. In general, it would be very difficult to find solutions in analytic form for such an equation. In the present study, we have been able to find different types of periodic and localized wave solutions by using an appropriate equation method. Remarkably, we have found that integration of Eq. (7) leads to physically relevant solutions satisfying the following equation:

$$\left(\frac{du}{d\xi} \right)^2 = a + bu^2 + cu^4. \tag{10}$$

The corresponding second- and fourth-order differential equations for $u(\xi)$ read

$$\frac{d^2 u}{d\xi^2} = bu + 2cu^3, \tag{11}$$

$$\frac{d^4 u}{d\xi^4} = (b^2 + 12ac)u + 20bcu^3 + 24c^2u^5. \tag{12}$$

The substitution of Eqs. (11) and (12) to Eq. (7) leads to the system of algebraic equations as

$$b^2 + 12ac + \lambda_0 b + \lambda_1 = 0, \tag{13}$$

$$20bc + 2\lambda_0 c + \lambda_2 = 0, \quad 24c^2 + \lambda_3 = 0. \tag{14}$$

The solution of these algebraic equations yields the parameters for Eq. (10) in an explicit form as

$$c = \pm \frac{1}{2} \sqrt{\frac{\mu}{6v}}, \quad b = \frac{\alpha}{10v} - \frac{3\rho^2}{80v^2} \mp \frac{\gamma}{10v} \sqrt{\frac{6v}{\mu}}, \tag{15}$$

$$a = \mp \frac{1}{6} \sqrt{\frac{6v}{\mu}} (\lambda_1 + \lambda_0 b + b^2). \tag{16}$$

Thus the parameters c , b , and a have two different forms with the top and bottom signs, respectively. The equation $d^3 u/d\xi^3 = (b + 6cu^2)du/d\xi$ follows from (11). We emphasize that substitution of this equation to (4) yields the relations given in Eq. (5) for arbitrary parameters b and c with $c \neq 0$ and nontrivial function $u(\xi)$ [$u(\xi) \neq \text{const}$].

We present below a number of periodic (or elliptic) solutions of the model (1) based on solving the nonlinear differential equation (10). These closed form solutions are expressed in terms of Jacobean elliptic functions of modulus k . We further show that special limiting cases of these families include the bright and dark solitary wave solutions.

III. PERIODIC AND SOLITARY WAVE SOLUTIONS

Before discussing the precise nature of periodic and solitary wave solutions of the model (1), we first consider the transformation of Eq. (10) based on function $y(\xi)$ as

$$u^2(\xi) = -\frac{1}{4c} y(\xi). \tag{17}$$

Thus we have found the nonlinear differential equation as

$$\left(\frac{dy}{d\xi} \right)^2 = f(y), \quad f(y) = \sigma_1 y + \sigma_2 y^2 - y^3, \tag{18}$$

where $\sigma_1 = -16ac$ and $\sigma_2 = 4b$. The function $f(y)$ can also be written in the form $f(y) = -y(y - y_-)(y - y_+)$, which yields the nonlinear differential equation

$$\left(\frac{dy}{d\xi} \right)^2 = -y(y - y_-)(y - y_+). \tag{19}$$

The polynomial $f(y)$ has three roots as

$$y_0 = 0, \quad y_{\pm} = 2(b \pm g), \quad g = \sqrt{b^2 - 4ac}. \tag{20}$$

Using the above results we present numerous periodic and solitary wave solutions for high dispersive cubic-quintic NLSE (1).

1. Periodic $(A + B \text{cn}^2)^{1/2}$ waves

We can order the roots of polynomial $f(y)$ as $y_1 < y_2 < y_3$, where $y_1 = y_0$, $y_2 = y_-$, and $y_3 = y_+$. In this case Eqs. (17) and (18) yield the periodic solution as

$$u(\xi) = \pm [A + B \text{cn}^2(w(\xi - \xi_0), k)]^{1/2}. \tag{21}$$

The parameters of this solution are

$$A = \frac{b(k^2 - 1)}{c(2 - k^2)}, \quad B = -\frac{bk^2}{c(2 - k^2)}, \tag{22}$$

$$w = \sqrt{\frac{b}{2 - k^2}}. \tag{23}$$

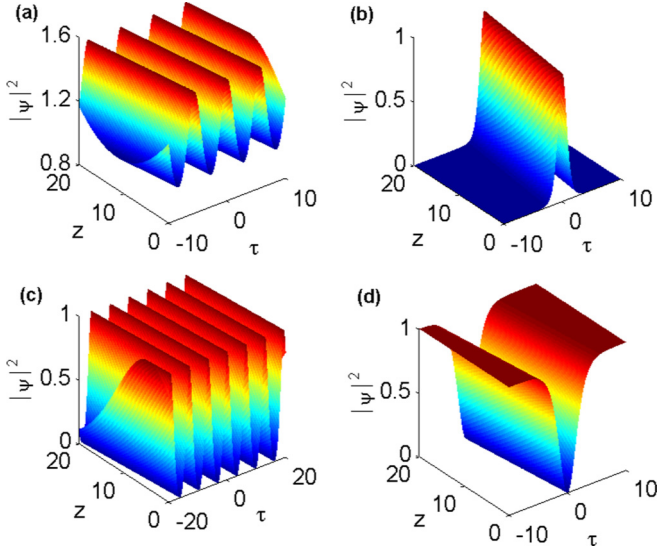


FIG. 1. Propagation of nonlinear waves (a) cn^2 -type periodic wave solution (25) with parameters $\rho = 0.25$, $\alpha = -0.3125$, $v = 0.25$, $\gamma = 1.5$, $\mu = 0.6144$, $\xi_0 = 0$, and $k = 0.6$, (b) bright solitary wave (28) with parameters $\alpha = 0.4$, $\rho = 1$, $v = 0.5$, $\gamma = 0.8$, $\mu = 0.75$, and $\xi_0 = 0$, (c) cn -type periodic wave (32) with parameters $\alpha = 0.25$, $\rho = 0.5$, $v = -0.5$, $\gamma = -0.56875$, $\mu = -0.75$, and $\xi_0 = 0$, and (d) dark solitary wave (36) with parameters $\alpha = 0.4$, $\rho = 1$, $v = 0.5$, $\gamma = 1.075$, $\mu = 0.75$, and $\xi_0 = 0$.

Here $\text{cn}(w(\xi - \xi_0), k)$ is Jacobi elliptic function where the modulus k belongs the interval $0 < k < 1$. The conditions for parameters as $b > 0$ and $c < 0$ follow from this solution. In this solution the parameter a depends on modulus k by relation as $a = b^2(1 - k^2)/c(2 - k^2)^2$. Thus the wave number κ by Eqs. (15) and (16) is

$$\kappa = b \left(\frac{3\rho^2}{8v} - \alpha \right) - \frac{\rho^2}{16v^2} \left(\frac{3\rho^2}{16v} - \alpha \right) + vb^2 + \frac{12vb^2(1 - k^2)}{(2 - k^2)^2}. \quad (24)$$

Substitution of the solution (21) into the wave function (2) yields the following family of periodic wave solutions for the high dispersive cubic-quintic NLSE (1):

$$\psi(z, \tau) = \pm [A + B \text{cn}^2(w(\xi - \xi_0), k)]^{1/2} \times \exp[i(\kappa z - \delta\tau + \theta)], \quad (25)$$

where modulus k is an arbitrary parameter in the interval $0 < k < 1$ and ξ_0 is the position of pulse at $z = 0$. We note that in the limiting cases with $k = 1$ this periodic wave reduces to a bright-type soliton solution. Figure 1(a) presents the evolution of the cn^2 -type periodic wave (25) for the physical parameter values $\rho = 0.25$, $\alpha = -0.3125$, $v = 0.25$, $\gamma = 1.5$, and $\mu = 0.6144$. To satisfy the parametric conditions $c < 0$ and $b^2 > 4ac$, we considered the case of bottom signs in all the parameters given in Eqs. (15) and (16). Also, the value of the elliptic modulus k is taken as $k = 0.6$. As concerns the inverse group velocity $q = v^{-1}$ of this cn^2 -type periodic wave, it can be determined from the relation (5) as $q = 0.1875$. Additionally, the position ξ_0 of the periodic waves at $z = 0$ is chosen to be equal to zero. As is seen from this figure, the

intensity profile presents an oscillating character which makes the wave a setting of light pulse train propagation in optical fibers. A particularly interesting property of this type of periodic waves is that its oscillating behavior is superimposed at a nonzero background, which is advantageous for a wide range of practical applications.

2. Bright solitary waves

We consider the limiting case of solution in Eq. (21) with $k = 1$. Thus we have the soliton solution of Eqs. (17) and (18) as

$$u(\xi) = \pm \left(-\frac{b}{c} \right)^{1/2} \text{sech}(\sqrt{b}(\xi - \xi_0)). \quad (26)$$

The condition $k = 1$ in Eq. (24) leads to the wave number κ as

$$\kappa = b \left(\frac{3\rho^2}{8v} - \alpha \right) - \frac{\rho^2}{16v^2} \left(\frac{3\rho^2}{16v} - \alpha \right) + vb^2. \quad (27)$$

Thus the bright solitary wave solution can be obtained for the high dispersive cubic-quintic NLSE (1) using Eqs. (2) and (26) as

$$\psi(z, \tau) = \pm \left(-\frac{b}{c} \right)^{1/2} \text{sech}(\sqrt{b}(\xi - \xi_0)) \times \exp[i(\kappa z - \delta\tau + \theta)], \quad (28)$$

with $b > 0$ and $c < 0$.

Figure 1(b) depicts the evolution of the intensity wave profile of the solitary wave solution (28) for the parameter values $\alpha = 0.4$, $\rho = 1$, $v = 0.5$, $\gamma = 0.8$, $\mu = 0.75$, and $\xi_0 = 0$. We have also considered the case of bottom signs in Eqs. (15) and (16) for the condition $c < 0$ to be fulfilled. It is interesting to see that this localized pulse exhibits a sech-type field profile like the traditional bright solitons of Kerr media.

3. Periodic cn waves

We can order the roots of polynomial $f(y)$ as $y_1 < y_2 < y_3$, where $y_1 = y_-$, $y_2 = y_0$, and $y_3 = y_+$. In this case Eqs. (17) and (18) yield the periodic solution as

$$u(\xi) = \pm \Lambda \text{cn}(w(\xi - \xi_0), k), \quad (29)$$

where the modulus k is an arbitrary parameter in the interval $0 < k < 1$. Here Λ and w are real parameters given by

$$\Lambda = \sqrt{\frac{-bk^2}{c(2k^2 - 1)}}, \quad w = \sqrt{\frac{b}{2k^2 - 1}}. \quad (30)$$

In this solution the parameter a depends on modulus k by relation as $a = b^2k^2(k^2 - 1)/c(2k^2 - 1)^2$. Thus the wave number κ by Eqs. (15) and (16) is

$$\kappa = b \left(\frac{3\rho^2}{8v} - \alpha \right) - \frac{\rho^2}{16v^2} \left(\frac{3\rho^2}{16v} - \alpha \right) + vb^2 + \frac{12vb^2k^2(k^2 - 1)}{(2k^2 - 1)^2}. \quad (31)$$

Substitution of the solution (29) into the wave function (2) yields the following family of periodic wave solutions for the

high dispersive cubic-quintic NLSE (1):

$$\psi(z, \tau) = \pm \Lambda \operatorname{cn}(w(\xi - \xi_0), k) \exp[i(\kappa z - \delta \tau + \theta)], \quad (32)$$

where modulus k is an arbitrary parameter in the interval $0 < k < 1$. The conditions for parameters as $b > 0$ and $c < 0$ follows from this solution. In the limiting case with $k = 1$ this solution reduces to the soliton solution given by Eq. (28).

In Fig. 1(c), we have shown the evolution of the cn-type periodic wave solution (32) for the parameter values $\alpha = 0.25$, $\rho = 0.5$, $\nu = -0.5$, $\gamma = -0.56875$, $\mu = -0.75$, and $\xi_0 = 0$. To satisfy the condition $c < 0$, we have considered the case of bottom signs in Eqs. (15) and (16). Unlike the periodic wave in (25), the periodic wave in the present case propagates on a zero background.

4. Dark solitary tanh waves

In the case with $g = 0$ or $b^2 = 4ac$ we can order the roots of polynomial $f(y)$ as $y_1 = y_2 < y_3$, where $y_1 = y_-, y_2 = y_+$, and $y_3 = y_0$. Note that for this case we have the condition $b < 0$. Thus the solution of Eqs. (17) and (18) has the kink wave solution as

$$u(\xi) = \pm \Lambda \tanh(w(\xi - \xi_0)). \quad (33)$$

The parameters of this solution are

$$\Lambda = \left(-\frac{b}{2c}\right)^{1/2}, \quad w = \frac{1}{2}\sqrt{-2b}, \quad (34)$$

where $b < 0$ and $c > 0$. The condition $b^2 = 4ac$ yields the wave number κ by Eqs. (15) and (16) as

$$\kappa = b\left(\frac{3\rho^2}{8\nu} - \alpha\right) - \frac{\rho^2}{16\nu^2}\left(\frac{3\rho^2}{16\nu} - \alpha\right) + 4\nu b^2. \quad (35)$$

Hence one obtains a kink solution for Eq. (1) of the form

$$\psi(z, \tau) = \pm \Lambda \tanh(w(\xi - \xi_0)) \exp[i(\kappa z - \delta \tau + \theta)]. \quad (36)$$

Note that this kink solution has the form of a dark soliton for intensity $I = |\psi(z, \tau)|^2 = \Lambda^2 \tanh^2(w(\xi - \xi_0))$.

Figure 1(d) displays the intensity profile of the solitary wave solution (36) for the parameter values $\alpha = 0.4$, $\rho = 1$, $\nu = 0.5$, $\gamma = 1.075$, $\mu = 0.75$, and $\xi_0 = 0$. To satisfy the conditions $b < 0$ and $c > 0$, we have considered the case of top signs in Eqs. (15) and (16).

5. Periodic sn/(1 + cn) waves

We have also found the periodic solution of Eq. (10) of the form

$$u(\xi) = \pm \frac{A \operatorname{sn}(w(\xi - \xi_0), k)}{1 + \operatorname{cn}(w(\xi - \xi_0), k)}. \quad (37)$$

The parameters for this periodic solution are

$$A = \sqrt{\frac{b}{2c(1 - 2k^2)}}, \quad w = \sqrt{\frac{2b}{1 - 2k^2}}, \quad (38)$$

where the modulus k is an arbitrary parameter for intervals $0 < k < 1/\sqrt{2}$ and $1/\sqrt{2} < k < 1$. The parameters of this solution are $b > 0$ and $c > 0$ when $0 < k < 1/\sqrt{2}$, and these parameters are $b < 0$ and $c > 0$ when $1/\sqrt{2} < k < 1$. This

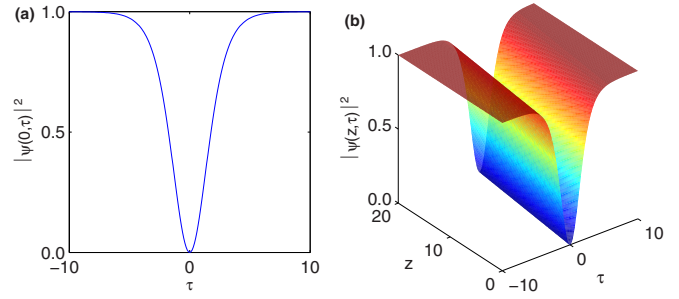


FIG. 2. (a) Intensity of the solitary wave profile $|\psi(0, \tau)|^2$ as a function of τ and its (b) evolution as computed from Eq. (41) for the values $\alpha = 0.4$, $\rho = 1$, $\nu = 0.5$, $\gamma = 1.075$, $\mu = 0.75$, and $\xi_0 = 0$.

solution takes place for condition $a = b^2/4c(1 - 2k^2)^2$, which yields the wave number κ by Eqs. (15) and (16) as

$$\kappa = b\left(\frac{3\rho^2}{8\nu} - \alpha\right) - \frac{\rho^2}{16\nu^2}\left(\frac{3\rho^2}{16\nu} - \alpha\right) + \nu b^2 + \frac{3\nu b^2}{(1 - 2k^2)^2}. \quad (39)$$

Now, taking into account the representation (2), the higher-order NLSE (1) has the following periodic wave solution:

$$\psi(z, \tau) = \pm \frac{A \operatorname{sn}(w(\xi - \xi_0), k)}{1 + \operatorname{cn}(w(\xi - \xi_0), k)} \exp[i(\kappa z - \delta \tau + \theta)]. \quad (40)$$

6. Dark solitary tanh/(1 + sech) waves

The limit $k \rightarrow 1$ in Eq. (40) leads to a solitary wave of the form

$$\psi(z, \tau) = \pm \frac{A_0 \tanh(w_0(\xi - \xi_0))}{1 + \operatorname{sech}(w_0(\xi - \xi_0))} \exp[i(\kappa z - \delta \tau + \theta)]. \quad (41)$$

The parameters for this solitary wave are

$$A_0 = \sqrt{-\frac{b}{2c}}, \quad w_0 = \sqrt{-2b}, \quad (42)$$

with $b < 0$ and $c > 0$ and $a = b^2/4c$. This solitary wave has the form of a dark soliton for intensity $I = |\psi(z, \tau)|^2$. The wave number κ for this solitary wave follows from Eq. (39) with $k = 1$:

$$\kappa = b\left(\frac{3\rho^2}{8\nu} - \alpha\right) - \frac{\rho^2}{16\nu^2}\left(\frac{3\rho^2}{16\nu} - \alpha\right) + 4\nu b^2. \quad (43)$$

Figure 2(a) presents the intensity profile of the optical solitary wave solution (41) for the parameter values $\alpha = 0.4$, $\rho = 1$, $\nu = 0.5$, $\gamma = 1.075$, $\mu = 0.75$, and $\xi_0 = 0$, while Fig. 2(b) shows its evolution. Here we considered the case of top signs in Eqs. (15) and (16). It is interesting to see that this nonlinear waveform is a dark solitary wave, which can be formed in the fiber medium due to a balance among all orders of dispersion up to the fourth order and both third- and fifth-order nonlinearities. Remarkably, the functional form of this solitary wave is different from the simplest dark solitary wave that has the form \tanh .

7. Periodic cn/(1 + sn) waves

We have found the periodic solution of Eq. (10) of the form

$$u(\xi) = \pm \frac{A \operatorname{cn}(w(\xi - \xi_0), k)}{1 + \operatorname{sn}(w(\xi - \xi_0), k)}, \tag{44}$$

where $0 < k < 1$. The parameters for this periodic solution are

$$A = \sqrt{\frac{b(1 - k^2)}{2c(1 + k^2)}}, \quad w = \sqrt{\frac{2b}{1 + k^2}}, \tag{45}$$

with $b > 0$ and $c > 0$. This solution takes place for condition $a = b^2(1 - k^2)^2/4c(1 + k^2)^2$, which yields the wave number κ by Eqs. (15) and (16) as

$$\begin{aligned} \kappa = b \left(\frac{3\rho^2}{8\nu} - \alpha \right) - \frac{\rho^2}{16\nu^2} \left(\frac{3\rho^2}{16\nu} - \alpha \right) \\ + \nu b^2 + \frac{3\nu b^2(1 - k^2)^2}{(1 + k^2)^2}. \end{aligned} \tag{46}$$

The substitution of solution (44) into Eq. (2) yields the family of periodic solutions for the higher-order NLSE (1) of the form

$$\psi(z, \tau) = \pm \frac{A \operatorname{cn}(w(\xi - \xi_0), k)}{1 + \operatorname{sn}(w(\xi - \xi_0), k)} \exp[i(\kappa z - \delta\tau + \theta)], \tag{47}$$

where modulus k is an arbitrary parameter in the interval $0 < k < 1$.

8. Periodic sn/(1 + dn) waves

We have found the exact periodic bounded solution of Eq. (10) of the form

$$u(\xi) = \pm \frac{A \operatorname{sn}(w(\xi - \xi_0), k)}{1 + \operatorname{dn}(w(\xi - \xi_0), k)}. \tag{48}$$

The parameters for this periodic solution are

$$A = \sqrt{\frac{-bk^4}{2c(2 - k^2)}}, \quad w = \sqrt{\frac{-2b}{2 - k^2}}, \tag{49}$$

where $b < 0$ and $c > 0$. This solution takes place for parameter $a = b^2k^4/4c(2 - k^2)^2$, which yields the wave number κ by Eqs. (15) and (16) as

$$\kappa = b \left(\frac{3\rho^2}{8\nu} - \alpha \right) - \frac{\rho^2}{16\nu^2} \left(\frac{3\rho^2}{16\nu} - \alpha \right) + \nu b^2 + \frac{3\nu b^2 k^4}{(2 - k^2)^2}. \tag{50}$$

Thus the appropriate periodic bounded solutions of Eq. (1) are

$$\psi(z, \tau) = \pm \frac{A \operatorname{sn}(w(\xi - \xi_0), k)}{1 + \operatorname{dn}(w(\xi - \xi_0), k)} \exp[i(\kappa z - \delta\tau + \theta)], \tag{51}$$

where modulus k is an arbitrary parameter in the interval $0 < k < 1$. It should be noticed that the limit $k \rightarrow 1$ in this solution yields the solitary wave solution given in Eq. (41).

An important finding is that the nonlinear waves given in this paper are stable and hence should be observable. The main interesting property of the reported structures is that

they propagate with a velocity which is uniquely dependent on all orders of dispersion up to the fourth order and is not affected by any nonlinearity parameter. Hence the velocity of the obtained propagating waves can be significantly reduced, enabling slow-light pulse propagation by appropriate manipulation of the dispersion parameters. This result may find application in developing slow-light systems [19]. Figure 3(a) depicts a typical example of the time evolution of intensity of the periodic wave (40) for the parameter values $\alpha = 1.64$, $\rho = -0.3$, $\nu = 1$, $\gamma = -0.1$, and $\mu = 1.5$. Then the velocity of the wave can be determined by using the relation (6) as $v \approx 4.12$. The results for the unbounded periodic wave (47) are illustrated in Fig. 3(b) for the values $\alpha = 0.305$, $\rho = -0.2$, $\nu = 0.5$, $\gamma = -1$, and $\mu = 0.3072$. The velocity of this wave can be calculated with the help of Eq. (6) resulting in $v \approx 17.54$. The intensity profile of the periodic wave solution (51) is shown in Fig. 3(c) for the values $\alpha = 0.21$, $\rho = -1$, $\nu = 1.5$, $\gamma = 1$, and $\mu = 0.0576$. Accordingly, the velocity of the wave is obtained as $v \approx 69.23$. Here we considered the case of top signs in all the parameters given in Eqs. (15) and (16) and the initial position ξ_0 of the periodic waves is chosen to be equal to zero. Also, the value of elliptic modulus k is taken as $k = 0.6$ for the solutions (40) and (47) and $k = 0.8$ for the solution (51). We can see from this figure that the profile of nonlinear waves presents the periodic property as it propagates through the optical fiber. It is also interesting to note that the oscillating behavior of this kind of periodic wave is superimposed at a zero background.

In view of the above results, we thus see that, in addition to the simplest periodic waves, periodic waves taking the forms (40), (41), (47), and (51) can also be formed in the fiber medium in the presence of various higher-order effects. This may be helpful for extending the applicability for periodic wave propagation through highly dispersive optical fibers. We should note here that the periodic structures are of increasing interest, particularly after the first experimental observation of the evolution of an arbitrarily shaped input optical pulse train to the shape preserving Jacobean elliptic pulse train corresponding to the Maxwell-Bloch equations [42]. Undoubtedly, such ultrashort solitary pulses could find potential applications in optical communication systems since dark solitons are more stable against Gordon-Haus jitters in a long communication line, less influenced by noise, and less sensitive to optical fiber loss [43,44].

Before we leave this section, we would like to compare the results presented in our study with those obtained for the generalized complex quintic Swift-Hohenberg (CQSH) equation [45], which models dissipative systems. The high dispersive cubic-quintic NLSE (1) presents an extra term with respect to the generalized CQSH equation, which is the third-order dispersion term $i\rho \frac{\partial^3 \psi}{\partial \tau^3}$. We have seen that this additional term has a significant influence on the characteristics of the obtained periodic and localized wave solutions. All the wave parameters (e.g., velocity, amplitude, inverse temporal width, and wave number) are dependent on the third-order dispersion coefficient ρ as well as the other system parameters. We should note here that all the involved coefficients in the CQSH model are complex parameters, unlike in the case of the model (1) where the equation parameters are real. The difference

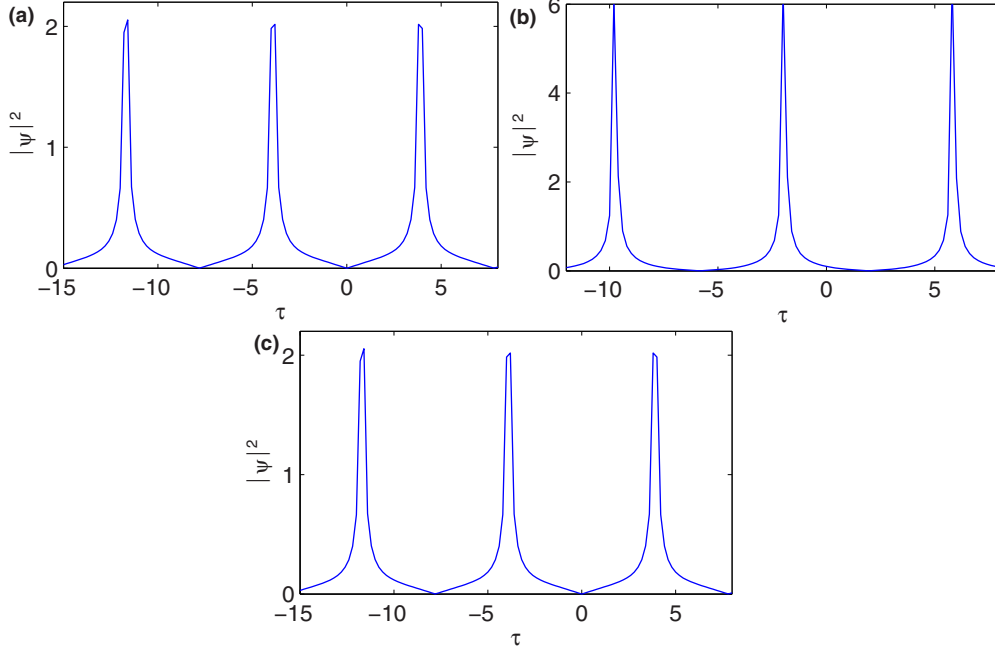


FIG. 3. Intensity profiles of (a) the periodic wave solution (40) with parameters $\alpha = 1.64$, $\rho = -0.3$, $\nu = 1$, $\gamma = -0.1$, $\mu = 1.5$, $\xi_0 = 0$, and $k = 0.6$, (b) the periodic wave solution (47) with parameters $\alpha = 0.305$, $\rho = -0.2$, $\nu = 0.5$, $\gamma = -1$, $\mu = 0.3072$, $\xi_0 = 0$, and $k = 0.6$, and (c) the periodic wave solution (51) with parameters $\alpha = 0.21$, $\rho = -1$, $\nu = 1.5$, $\gamma = 1$, $\mu = 0.0576$, $\xi_0 = 0$, and $k = 0.8$.

in the nature of coefficients in the two models defines the dissimilarity in the behavior of the propagating waves. For instance, it is found that the CQSH model admits a bright soliton solution with a sech-type wave form [see Eq. (73) in Ref. [45]] but the parameters of this solution such as phase, amplitude, and width are markedly different from those in the bright solitary wave (28).

IV. ANALYTICAL STABILITY ANALYSIS

We present in this section the stability analysis of the high dispersive cubic-quintic NLSE (1). Our approach is based on the theory of optical nonlinear dispersive waves [20]. We develop the dynamics of nonlinear dispersive waves in the form

$$\psi(z, \tau) = U(\omega) \exp[i\Theta(z, \tau)], \quad (52)$$

where the amplitude $U(\omega)$ and phase $\Theta(z, \tau)$ are the real functions. We define the wave number $k(z, \tau)$ and frequency $\omega(z, \tau)$ of the nonlinear dispersive waves by equations

$$k(z, \tau) = \frac{\partial \Theta(z, \tau)}{\partial z}, \quad \omega(z, \tau) = -\frac{\partial \Theta(z, \tau)}{\partial \tau}. \quad (53)$$

We also assume here that the functions $k(z, \tau)$ and $\omega(z, \tau)$ are slowly varying functions of slow variables $Z = \varepsilon z$ and $T = \varepsilon \tau$: $k(z, \tau) = \bar{k}(Z, T)$ and $\omega(z, \tau) = \bar{\omega}(Z, T)$, where $\varepsilon \ll 1$. We note that the dimensionless small parameter ε is the same as that used for derivation of high dispersive cubic-quintic NLSE (1) in the approximation of slowly varying amplitude $\psi(z, \tau)$ [2]. The substitution of Eq. (52) to generalized NLSE (1) yields the series of nonlinear equations. Two equation in

zero and first order to small parameter ε can be written in the form

$$k(\omega) = k_0(\omega) + \gamma U^2(\omega) - \mu U^4(\omega),$$

$$k_0(\omega) = \alpha \omega^2 + \rho \omega^3 + \nu \omega^4, \quad (54)$$

$$\frac{\partial}{\partial z} U^2(\omega) + \frac{\partial}{\partial \tau} [k'_0(\omega) U^2(\omega)] = 0, \quad (55)$$

where $k'_0(\omega) = dk_0(\omega)/d\omega$. Here Eq. (54) is the nonlinear dispersion equation and Eq. (55) describes the evolution of amplitude $U(\omega)$. Using Eq. (53) we have the relations as $\Theta_{z\tau} = k_\tau$ and $\Theta_{\tau z} = -\omega_z$. Thus the relation $\Theta_{z\tau} = \Theta_{\tau z}$ leads to the equation for varying frequency $\omega(z, \tau)$ and wave number $k(z, \tau)$ as

$$\frac{\partial \omega(z, \tau)}{\partial z} + \frac{\partial k(z, \tau)}{\partial \tau} = 0. \quad (56)$$

Using Eq. (54) and relation $U_\tau = U' \omega_\tau$ (with $U' = dU/d\omega$) we can rewrite Eqs. (55) and (56) in the following form:

$$\frac{\partial U}{\partial z} + k'(\omega) \frac{\partial U}{\partial \tau}$$

$$= -\frac{1}{2} k''_0(\omega) U \frac{\partial \omega}{\partial \tau} + (2\gamma U - 4\mu U^3) (U')^2 \frac{\partial \omega}{\partial \tau}, \quad (57)$$

$$\frac{\partial \omega}{\partial z} + k'(\omega) \frac{\partial \omega}{\partial \tau} = 0, \quad (58)$$

where $k'(\omega) = k'_0(\omega) + (2\gamma U - 4\mu U^3) U'$. This system of equations can be hyperbolic or elliptic. We first consider the case when this system of equations is hyperbolic. The

characteristics to the hyperbolic system of Eqs. (57) and (58) are given by

$$\frac{dU}{dz} = -\frac{1}{2}k_0''(\omega)U \frac{\partial\omega}{\partial\tau} + (2\gamma U - 4\mu U^3)(U')^2 \frac{\partial\omega}{\partial\tau}, \quad (59)$$

$$\frac{d\omega}{dz} = 0, \quad \frac{d\tau}{dz} = k'(\omega). \quad (60)$$

The relation $dU/dz = U'd\omega/dz = 0$ follows from Eq. (60). Hence Eq. (59) leads to the nonlinear differential equation as

$$(\gamma - 2\mu U^2) \left(\frac{dU}{d\omega}\right)^2 = \frac{1}{4}k_0''(\omega), \quad (61)$$

$$k_0''(\omega) = 2\alpha + 6\rho\omega + 12v\omega^2.$$

Thus Eqs. (60) and (61) lead to the following characteristic equation:

$$\frac{d\tau}{dz} = k_0'(\omega) \pm [\gamma U(\omega) - 2\mu U^3(\omega)] \times \sqrt{\frac{k_0''(\omega)}{\gamma[1 - 2(\mu/\gamma)U^2(\omega)]}}. \quad (62)$$

The functions $k_0'(\omega)$ and $k_0''(\omega)$ for $\omega = \delta = -\rho/4v$ are

$$k_0'(\delta) = \frac{\rho(\rho^2 - 4\alpha v)}{8v^2} = v^{-1}, \quad k_0''(\delta) = \frac{8\alpha v - 3\rho^2}{4v}. \quad (63)$$

Thus the characteristic in Eq. (62) at $\omega = \delta$ is given by

$$\frac{d\tau}{dz} = v^{-1} \pm \frac{1}{2}[\gamma U(\delta) - 2\mu U^3(\delta)] \times \sqrt{\frac{8\alpha v - 3\rho^2}{v\gamma[1 - 2(\mu/\gamma)U^2(\delta)]}}. \quad (64)$$

The wave solutions of generalized NLSE (1) are stable when they cannot radiate the nonlinear dispersive waves. Moreover, the outgoing nonlinear dispersive waves exist only in the case when the system of Eqs. (57) and (58) is hyperbolic [20]. We emphasize that in the case of elliptic equations the problem of optical pulse radiation is not correct from the mathematical point of view. The system of Eqs. (57) and (58) is elliptic when the square root in Eq. (62) is imaginary because in this case the characteristics given by Eqs. (59) and (60) do not exist.

Thus it follows from (64) that the criterion of stability of solutions for generalized NLSE (1) at $\omega = \delta$ is

$$\frac{8\alpha v - 3\rho^2}{v\gamma[1 - 2(\mu/\gamma)U^2(\delta)]} < 0. \quad (65)$$

We have two cases for the stability criterion of solutions of Eq. (65). In the first case we assume $\mu/\gamma < 0$ and hence the criterion of stability is given by

$$\frac{8\alpha v - 3\rho^2}{v\gamma} < 0. \quad (66)$$

In the second case with $\mu/\gamma > 0$ we assume that $U^2(\delta) < \gamma/2\mu$. This case occurs for appropriate realistic values of parameter $\gamma/2\mu$ because the intensity $I = U^2(\delta)$ of dispersive waves is sufficiently small. Thus, in this second case, the criterion of stability of solutions is given by Eq. (66)

as well. However, we note that in the case when $\mu/\gamma > 0$ and $U^2(\delta) > \gamma/2\mu$ the stability criterion has the following form: $(8\alpha v - 3\rho^2)/v\gamma > 0$. We present below the domains of parameters for which the solutions 1–8 are stable. These domains are found using appropriate conditions for parameters b and c and the stability criterion given in Eq. (66).

(1) *Stability condition for solutions with $b > 0$ and $c < 0$.* The solutions 1–3 are found for parameters $b > 0$ and $c < 0$. It follows from Eq. (15) that $\mu/v > 0$ and $c = -(1/2)\sqrt{\mu/6v}$. Hence we should use in Eq. (15) the bottom signs. The condition $b > 0$ yields the relation

$$8\alpha v - 3\rho^2 > -8v\gamma \sqrt{\frac{6v}{\mu}}. \quad (67)$$

Thus Eqs. (66) and (67) lead in the first case [with $v\gamma > 0$ and $\mu/v > 0$] the stability condition for solutions 1–3 as

$$-8\sqrt{\frac{6v}{\mu}} < \frac{8\alpha v - 3\rho^2}{v\gamma} < 0. \quad (68)$$

In the second case (with $v\gamma < 0$ and $\mu/v > 0$) Eqs. (66) and (67) yield the stability condition for solutions 1–3 as

$$\frac{8\alpha v - 3\rho^2}{v\gamma} < -8\sqrt{\frac{6v}{\mu}}. \quad (69)$$

(2) *Stability condition for solutions with $b < 0$ and $c > 0$.* The solutions 4, 6, 8, and 5 (in the domain $1/\sqrt{2} < k < 1$ of modulus k) are found for parameters $b < 0$ and $c > 0$. It follows from Eq. (15) that $\mu/v > 0$ and $c = (1/2)\sqrt{\mu/6v}$. Hence we should use in Eq. (15) the top signs. The condition $b < 0$ yields relation

$$8\alpha v - 3\rho^2 < 8v\gamma \sqrt{\frac{6v}{\mu}}. \quad (70)$$

Hence Eqs. (66) and (70) lead in the first case (with $v\gamma > 0$ and $\mu/v > 0$) the stability condition for solutions 4, 6, 8, and 5 (in the domain $1/\sqrt{2} < k < 1$ of modulus k) as

$$\frac{8\alpha v - 3\rho^2}{v\gamma} < 0. \quad (71)$$

In the second case (with $v\gamma < 0$ and $\mu/v > 0$) Eq. (70) yields $(8\alpha v - 3\rho^2)/v\gamma > 8\sqrt{6v/\mu}$. However, this inequality disagrees with stability criterion in Eq. (66). Thus in this second case (with $v\gamma < 0$ and $\mu/v > 0$) the solutions 4, 6, 8, and 5 (in the domain $1/\sqrt{2} < k < 1$ of modulus k) are unstable.

(3) *Stability condition for solutions with $b > 0$ and $c > 0$.* The solutions 7 and 5 (in the domain $0 < k < 1/\sqrt{2}$ of modulus k) are found for parameters $b > 0$ and $c > 0$. It follows from Eq. (15) that $\mu/v > 0$ and $c = (1/2)\sqrt{\mu/6v}$. Hence we should use in Eq. (15) the top signs. The condition $b > 0$ yields relation

$$8\alpha v - 3\rho^2 > 8v\gamma \sqrt{\frac{6v}{\mu}}. \quad (72)$$

In the first case (with $\nu\gamma > 0$ and $\mu/\nu > 0$) Eq. (72) yields $(8\alpha\nu - 3\rho^2)/\nu\gamma > 8\sqrt{6\nu/\mu}$. This inequality disagrees with stability criterion in Eq. (66). Thus in the first case (with $\nu\gamma > 0$ and $\mu/\nu > 0$) the solutions 7 and 5 (in the domain $0 < k < 1/\sqrt{2}$ of modulus k) are unstable.

In the second case (with $\nu\gamma < 0$ and $\mu/\nu > 0$) Eqs. (66) and (72) yield the stability condition for solutions 7 and 5 (in the domain $0 < k < 1/\sqrt{2}$ of modulus k) as

$$\frac{8\alpha\nu - 3\rho^2}{\nu\gamma} < 0. \quad (73)$$

In the conclusion, we note that the numerical stability analysis presented in the following section is consistent with analytical criteria developed here.

V. NUMERICAL STABILITY ANALYSIS

We now employ the direct numerical simulations to verify the stability of our analytical solutions against small perturbations. It is observed that competing nonlinearities which occur in a cubic-quintic nonlinear optical medium can lead to stabilization of soliton solutions [16]. The present higher-order NLSE (1) includes the contribution of such cubic-quintic nonlinearity in addition to the effects of second-, third-, and fourth-order dispersions. In order to strictly answer the question of robustness of the obtained solutions, much further analysis is needed which we have presented below.

To examine stability with respect to finite perturbations for the solutions, we take as examples the first types of periodic wave (25), bright solitary wave (28), and dark solitary wave (36). Then, we perform a direct numerical simulation of Eq. (1) using the standard split-step Fourier method [46], to test the stability of solutions (25), (28), and (36) with initial white noise, as compared to Figs. 1(a), 1(b), and 1(d). As usual, we put the noise onto the initial profile; then the perturbed pulse reads [47] $\psi_{\text{pert}} = \psi(\tau, 0)[1 + 0.1 \text{random}(\tau)]$. The numerical results of periodic wave, bright, and dark solitary wave solutions under the perturbation of 10% white noise are displayed in Figs. 4(a), 4(b), and 4(c), respectively. From Fig. 4, we can see that under finite initial perturbations of the additive white noise, the solitary and periodic waves still propagate in a stable way, thereby further confirming the validity of our solutions. Although we have shown here the results of stability study only for three examples of NLSE model (1), similar conclusions hold for other solutions as well. Therefore, we can conclude that the solutions we obtained are stable and should be observable in optical cubic-quintic materials with higher-order dispersion.

VI. DISCUSSION

Before arriving at a conclusion, let us discuss some practical application of the considered theoretical model. With the rapid advancement in optical materials research and availability of high power laser systems, there are new photonic waveguides that show complicated dispersion and nonlinear properties. For instance, it was reported recently that it is possible to realize a pure quartic soliton just by the balance of the nonlinearity with higher-order dispersion of order four [48]. The authors experimentally demonstrated the existence

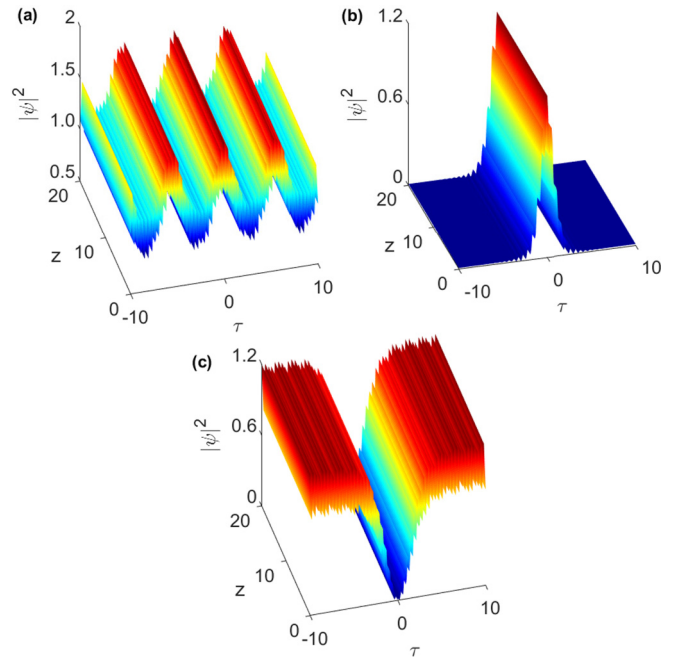


FIG. 4. Numerical evolution of (a) the periodic wave solution (25), (b) the bright solitary wave solution (28), and (c) the dark solitary wave solution (36) under the perturbation of white noise whose maximal value is 0.1. The parameters are the same as in Figs. 1(a), 1(b), and 1(d), respectively.

of pure-quartic solitons in a silicon photonic crystal waveguide (PhC-wg) at a carrier frequency where the quadratic and cubic dispersion parameters β_2 and β_3 were practically negligible. Such waveguides exhibit fourth-order dispersion and researchers successfully demonstrated various nonlinear phenomenalike pulse compression, slow light degeneration [49,50], etc.

Recently, Roy and Biancalana [51] demonstrated that it is possible to observe quartic solitons in specially designed silicon-based waveguides when both β_2 and the quartic dispersion parameter β_4 are negative (anomalous). By considering the case when β_4 is negative and β_2 can have either sign, Tam *et al.* [52] numerically found that single-hump solitons exist for some positive β_2 values as well. The existence of quartic solitons in the presence of third-order dispersion (i.e., $\beta_3 \neq 0$), for which the phase depends on the time variable, was recently reported by Kruglov and Harvey [19], who found the stability region of this class of solitons as $\beta_2 < 0$, $\beta_4 < 0$, and $2\beta_2\beta_4 > \beta_3^2$. At this point it should be noted that such dependence of the phase on time τ can be interpreted as a shift $\Delta\omega$ in the carrier frequency away from the expansion frequency ω_0 , where the three dispersion parameters β_2 , β_3 , and β_4 were defined by Taylor expansion [52]. According to these recent works, the formation of temporal solitons arises from the interplay between Kerr nonlinearity and all orders of dispersion up to the fourth order.

But when the power of the light pulse exceeds a threshold value, the quintic nonlinearity coming from fifth-order susceptibility contributes significantly in the nonlinear response of the medium and at the same time the effect of higher-order dispersion cannot be neglected [53]. In this context,

considering the combined influence of third-order dispersion and cubic-quintic nonlinearity, results showing the pulse evolution in a non-Kerr type medium have been recently reported [53]. It is noteworthy that for such cubic-quintic media, the nonlinear change in the refractive index of optical media can be modeled by a linear and quadratic dependence on wave intensity as [54] $\Delta n = n_2|E|^2 + n_4|E|^4$, which with negative nonlinear coefficients $n_2 n_4 < 0$ results in bistable soliton propagation [55,56]. Note that here the nonlinear refractive indices n_2 and n_4 are proportional to the third- [$\chi^{(3)}$] and fifth-order [$\chi^{(5)}$] nonlinear susceptibilities, respectively, as [56] $n_2 = 3\chi^{(3)}/(8n_0)$ and $n_4 = 5\chi^{(5)}/(16n_0)$, with n_0 being the linear refractive index coefficient. This change in the refractive index indicates that the quintic nonlinearity plays a crucial role in the response of the system.

Considering the fact that the silicon photonic crystal waveguide (PhC-wg) allow for the most degrees of freedom in dispersion engineering [57,58], this medium is also able to support quintic nonlinearity by appropriately exciting it with suitable high powers. It is relevant to note that, for the up to the fourth-order dispersion and the quintic nonlinearity to be taken into account, the light pulse should be extremely narrow and the optical intensity should be very high [59].

Now we consider a limit when solutions of Ref. [19] are recovered. This is connected with a condition which permits one to neglect the last term in Eq. (1). It is apparent that such condition is given by $(|\mu|/|\gamma|)|\psi(z, \tau)|^2 \ll 1$, which can also be written as $|\mu|I_m \ll |\gamma|$, where $I_m = \max|\psi(z, \tau)|^2$ is the maximal intensity of optical pulse. It is relevant to mention that appropriate scaling of Eq. (1) leads to a two-parameter canonical form of generalized NLSE, which allows one to formulate the above condition in a different form (see the Appendix).

For the completeness of the investigation, we now discuss the influence of quintic nonlinearity on the dynamical behaviors of the obtained periodic and localized waves. Here we still take the periodic wave (25), bright solitary wave (28), and dark solitary wave (36) as examples to study the effect of quintic nonlinearity on the dynamical properties of the derived structures. From the above results, we see that the quintic nonlinearity coefficient μ included in the parameters b and c affects the width, amplitude, and wave number of the obtained propagating waves. It should be noted that these wave parameters take nonzero values only for $b \neq 0$ and $c \neq 0$ (i.e., $\mu \neq 0$). In Fig. 5, we have shown the temporal intensity profiles of the nonlinear wave solutions (25), (28), and (36) for different values of μ and $\alpha = 0.2$, $\rho = 0.4$, $\nu = 0.1$, and $\gamma = 1$. Here, the value of the elliptic modulus k is taken as $k = 0.6$ for the cn^2 periodic wave (25) and ξ_0 is chosen to be equal to zero. Also we considered the case of bottom signs in all the parameters given in Eqs. (15) and (16) for the periodic and bright solitary wave solutions (25) and (28), while the top signs are considered for the dark solitary wave solution (36). From Figs. 5(a) and 5(b), one can observe that, with increasing the quintic nonlinearity parameter μ , the intensity of the periodic and bright solitary waves decreases continuously. We also see that this parameter influences the background intensity of the dark solitary wave, as shown in Fig. 5(c). We can then conclude that the

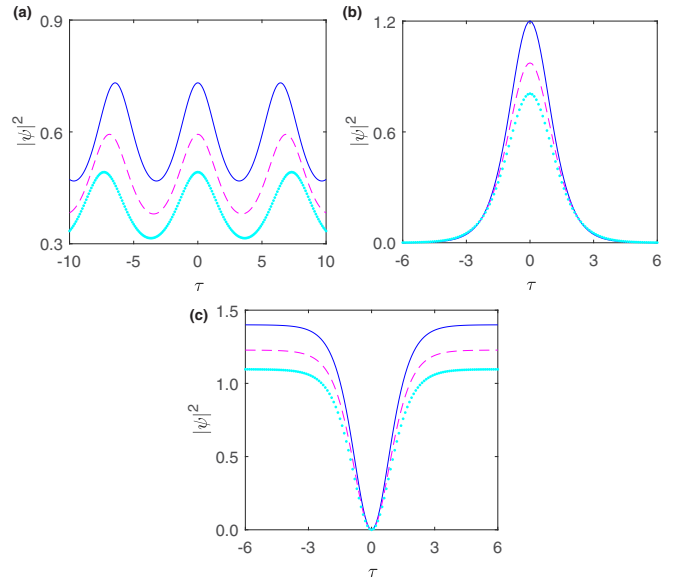


FIG. 5. Intensity profiles of the (a) periodic wave (25), (b) bright solitary wave (28), and (c) dark solitary wave (36) for different values of μ : $\mu = 0.6$ (thick line), $\mu = 0.7$ (dashed line), and $\mu = 0.8$ (dotted line). The selected coefficients are $\alpha = 0.2$, $\rho = 0.4$, $\nu = 0.1$, and $\gamma = 1$.

quintic nonlinearity plays a sensitive role in the evolutionary dynamics of propagating waves.

VII. CONCLUSION

We have studied the femtosecond light pulse propagation in a highly dispersive optical fiber governed by a higher-order nonlinear Schrödinger equation incorporating all orders of dispersion up to the fourth order as well as cubic and quintic nonlinearities. With use of an appropriate equation, exact periodic wave solutions have been identified for the model in the presence of various dispersive and nonlinear effects. Solitary waves have been also obtained which include both bright and dark localized solutions. It is found that the velocity of these structures is uniquely dependent on all orders of dispersion. Moreover, all solutions presented in the paper are stable to small perturbations which follows from appropriate stability analysis. The conditions on the optical fiber parameters for the existence of these exact stable solutions are found by analytical stability analysis as well. It is apparent that the exact nature of the nonlinear waves presented here can lead to different applications in optical communications.

APPENDIX: DIMENSIONLESS FORM OF GENERALIZED NLSE

We present in this Appendix the scaling of Eq. (1) leading to the dimensionless form of generalized NLSE. Thus we define the complex field envelope as $\psi(z, \tau) = QU(\zeta, \xi)$, where $U(\zeta, \xi)$ is a dimensionless complex valued function and the dimensionless variables are $\zeta = z/L$ and $\xi = \tau/T$. We also define here the characteristic length L , time T , and

amplitude Q as

$$L = \frac{\rho^2}{|\alpha|^3}, \quad T = \frac{|\rho|}{|\alpha|}, \quad Q = \frac{|\alpha|}{|\rho|} \sqrt{\frac{|\alpha|}{|\gamma|}}. \quad (\text{A1})$$

The above definitions lead to a two-parameter canonical form of generalized NLSE given by

$$i \frac{\partial U}{\partial \zeta} = S(\alpha) \frac{\partial^2 U}{\partial \xi^2} + i S(\rho) \frac{\partial^3 U}{\partial \xi^3} - \sigma \frac{\partial^4 U}{\partial \xi^4} - S(\gamma) |U|^2 U + \lambda |U|^4 U, \quad (\text{A2})$$

where $S(\alpha) \equiv \text{sgn}(\alpha)$, $S(\rho) \equiv \text{sgn}(\rho)$, and $S(\gamma) \equiv \text{sgn}(\gamma)$. Thus we have $S(\alpha) = \frac{\alpha}{|\alpha|}$, $S(\rho) = \frac{\rho}{|\rho|}$, and $S(\gamma) = \frac{\gamma}{|\gamma|}$, where it is assumed that $\alpha \neq 0$, $\rho \neq 0$, and $\gamma \neq 0$. Hence the parameters $S(\alpha)$, $S(\rho)$, and $S(\gamma)$ in this dimensionless NLSE can

accept only two values as ± 1 . The dimensionless parameters σ and λ are given here as

$$\sigma = \frac{\nu |\alpha|}{\rho^2}, \quad \lambda = \frac{\mu |\alpha|^3}{\gamma^2 \rho^2}. \quad (\text{A3})$$

It follows from Eq. (A2) that one can neglect the last term in this equation when the condition $|\lambda| |U|^2 \ll 1$ is satisfied. This condition can also be written as

$$|\mu| |\alpha|^3 J_m \ll \gamma^2 \rho^2, \quad (\text{A4})$$

with $J_m = \max |U(\zeta, \xi)|^2$. However, a more precise condition allowing one to neglect the last term in Eq. (A2) with fixed parameters $\alpha, \rho, \nu, \gamma, \mu$ and for initial complex field $U(0, \xi)$ can be found by numerical simulations of (A2).

[1] Yu. S. Kivshar and G. P. Agrawal, *Optical Solitons: From Fibers to Photonic Crystals* (Academic, New York, 2003).

[2] G. P. Agrawal, *Applications of Nonlinear Fiber Optics* (Academic, San Diego, 2001).

[3] Alka, A. Goyal, R. Gupta, C. N. Kumar, and T. S. Raju, *Phys. Rev. A* **84**, 063830 (2011).

[4] A. Choudhuri and K. Porsezian, *Opt. Commun.* **285**, 364 (2012).

[5] Z. H. Li, L. Li, H. Tian, and G. S. Zhou, *Phys. Rev. Lett.* **84**, 4096 (2000).

[6] H. Triki, F. Azzouzi, and Ph. Grelu, *Opt. Commun.* **309**, 71 (2013).

[7] A. Biswas and S. Konar, *Introduction to Non-Kerr Law Optical Solitons* (Chapman & Hall, London, 2003).

[8] M. Kolesik and J. V. Moloney, *Rep. Prog. Phys.* **77**, 016401 (2014).

[9] C. Zhan, D. Zhang, D. Zhu, D. Wang, Y. Li, D. Li, Z. Lu, L. Zhao, and Y. Nie, *J. Opt. Soc. Am. B* **19**, 369 (2002); B. L. Lawrence, M. Cha, W. E. Torruellas, G. I. Stegeman, S. Etemad, G. Baker, and F. Kajzar, *Appl. Phys. Lett.* **64**, 2773 (1994).

[10] J. L. Coutaz and M. Kull, *J. Opt. Soc. Am. B* **8**, 95 (1991).

[11] A. S. Reyna, E. Bergmann, P.-F. Brevet, and C. B. de Araújo, *Opt. Express* **25**, 21049 (2017).

[12] P. B ejot, J. Kasparian, S. Henin, V. Loriot, T. Vieillard, E. Hertz, O. Faucher, B. Lavorel, and J.-P. Wolf, *Phys. Rev. Lett.* **104**, 103903 (2010); C. Br ee, A. Demircan, and G. Steinmeyer, *ibid.* **106**, 183902 (2011); G. Point, Y. Brelet, A. Houard, V. Jukna, C. Milian, J. Carbonnel, Y. Liu, A. Couairon, and A. Mysyrowicz, *ibid.* **112**, 223902 (2014).

[13] P. B ejot, E. Hertz, B. Lavorel, J. Kasparian, J.-P. Wolf, and O. Faucher, *Opt. Lett.* **36**, 828 (2011); M. Bache, F. Eilenberger, and S. Minardi, *ibid.* **37**, 4612 (2012); D. L. Weerawarne, X. Gao, A. L. Gaeta, and B. Shim, *Phys. Rev. Lett.* **114**, 093901 (2015).

[14] L. Hong, H. Xian-Tu, and L. Sen-Yue, *Chin. Phys. Lett.* **19**, 87 (2002).

[15] G. S. Parmar, S. Jana, and B. A. Malomed, *J. Opt. Soc. Am. B* **34**, 850 (2017).

[16] M. Quiroga-Teixeiro and H. Michinel, *J. Opt. Soc. Am. B* **14**, 2004 (1997).

[17] J. M. Soto-Crespo and N. Akhmediev, *J. Opt. Soc. Am. B* **38**, 3541 (2021).

[18] M. Saha and A. K. Sarma, *Opt. Commun.* **291**, 321 (2013); Y. Liu, Y. L. Xue, and C. Yu, *ibid.* **339**, 66 (2015).

[19] V. I. Kruglov and J. D. Harvey, *Phys. Rev. A* **98**, 063811 (2018).

[20] H. Triki and V. I. Kruglov, *Phys. Rev. E* **101**, 042220 (2020).

[21] V. I. Kruglov and H. Triki, *Phys. Rev. A* **102**, 043509 (2020).

[22] C. Q. Dai, Y. Y. Wang, and C. Yan, *Opt. Commun.* **283**, 1489 (2010).

[23] V. M. Petnikova, V. V. Shuvalov, and V. A. Vysloukh, *Phys. Rev. E* **60**, 1009 (1999).

[24] K. W. Chow, K. Nakkeeran, and B. A. Malomed, *Opt. Commun.* **219**, 251 (2003).

[25] K. W. Chow, I. M. Merhasin, B. A. Malomed, K. Nakkeeran, K. Senthilnathan, and P. K. A. Wai, *Phys. Rev. E* **77**, 026602 (2008).

[26] F. Kh. Abdullaev, A. M. Kamchatnov, V. V. Konotop, and V. A. Brazhnyi, *Phys. Rev. Lett.* **90**, 230402 (2003).

[27] Z. Yan, K. W. Chow, and B. A. Malomed, *Chaos Solitons & Fractals* **42**, 3013 (2009).

[28] A. Joseph and K. Porsezian, *J. Nonlinear Opt. Phys. & Mater.* **19**, 177 (2010).

[29] H. Triki and V. I. Kruglov, *Opt. Commun.* **502**, 127409 (2022).

[30] H. Triki and V. I. Kruglov, *Chaos Solitons & Fractals* **153**, 111496 (2021).

[31] S. L. Palacios and J. M. Fern andez-D ıaz, *Opt. Commun.* **178**, 457 (2000).

[32] Y. Xie, Z. Yang, and L. Li, *Phys. Lett. A* **382**, 2506 (2018).

[33] Y. Xie and S. Tang, *J. Appl. Math.* **2014**, 826746 (2014).

[34] L. Hua-Mei, X. You-Shen, and L. Ji, *Commun. Theor. Phys.* **41**, 829 (2004).

[35] A. M. Sultan, D. Lu, M. Arshad, H. U. Rehman, and M. S. Saleem, *Chin. J. Phys.* **67**, 405 (2020).

[36] K. Hosseini, R. Ansari, F. Samadani, A. Zabihi, A. Shafaroody, and M. Mirzazadeh, *Acta Phys. Pol. A* **136**, 203 (2019).

[37] G. P. Agrawal and C. Headley, III, *Phys. Rev. A* **46**, 1573 (1992).

- [38] Y.-F. Chen, K. Beckwitt, F. W. Wise, B. G. Aitken, J. S. Sanghera, and I. D. Aggarwal, *J. Opt. Soc. Am. B* **23**, 347 (2006).
- [39] B. Lawrence, W. E. Torruellas, M. Cha, M. L. Sundheimer, G. I. Stegeman, J. Meth, S. Etemad, and G. Baker, *Phys. Rev. Lett.* **73**, 597 (1994); B. L. Lawrence, M. Cha, J. U. Kang, W. Toruellas, G. Stegeman, G. Baker, J. Meth, and S. Etemad, *Electron. Lett.* **30**, 447 (1994).
- [40] P. Roussignol, D. Ricard, J. Lukasik, and C. Flytzanis, *J. Opt. Soc. Am. B* **4**, 5 (1987); L. H. Acioli, A. S. L. Gomes, J. M. Hickmann, and C. B. de Araujo, *Appl. Phys. Lett.* **56**, 2279 (1990); F. Lederer and W. Biehlig, *Electron. Lett.* **30**, 1871 (1994).
- [41] J. F. Zhang, Q. Tian, Y. Y. Wang, C. Q. Dai, and L. Wu, *Phys. Rev. A* **81**, 023832 (2010).
- [42] J. L. Shultz and G. J. Salamo, *Phys. Rev. Lett.* **78**, 855 (1997).
- [43] S. Yu. Kivshar, M. Haelterman, Ph. Emplit, and J. P. Hamaide, *Opt. Lett.* **19**, 786 (1994).
- [44] A. Choudhuri and K. Porsezian, *Phys. Rev. A* **88**, 033808 (2013).
- [45] K.-i. Maruno, A. Ankiewicz, and N. Akhmediev, *Physica D* **176**, 44 (2003).
- [46] G. P. Agrawal, *Nonlinear Fiber Optics*, 4th ed. (Academic, Boston, 2006), Chap. 2.
- [47] J. R. He and H. M. Li, *Phys. Rev. E* **83**, 066607 (2011).
- [48] A. Blanco-Redondo, C. M. de Sterke, J. E. Sipe, T. F. Krauss, B. J. Eggleton, and C. Husko, *Nat. Commun.* **7**, 10427 (2016).
- [49] J. Li, L. O'Faolain, I. H. Rey, and T. F. Krauss, *Opt. Express* **19**, 4458 (2011).
- [50] B. J. Soller, D. K. Gifford, M. S. Wolfe, and M. E. Froggatt, *Opt. Express* **13**, 666 (2005).
- [51] S. Roy and F. Biancalana, *Phys. Rev. A* **87**, 025801 (2013).
- [52] K. K. K. Tam, T. J. Alexander, A. Blanco-Redondo, and C. M. de Sterke, *Phys. Rev. A* **101**, 043822 (2020).
- [53] S. Roy and S. Bhadra, *J. Nonlinear Opt. Phys. Mater.* **16**, 119 (2007).
- [54] A. S. Bezerra Sombra, *Opt. Commun.* **94**, 92 (1992).
- [55] J. Herrmann, *Opt. Commun.* **87**, 161 (1992).
- [56] S. Tanev and D. I. Pushkarov, *Opt. Commun.* **141**, 322 (1997).
- [57] B. Kuyken, F. Leo, S. Clemmen, U. Dave, R. Van Laer, T. Ideguchi, H. Zhao, X. Liu, J. Safioui, S. Coen, S. P. Gorza, S. K. Selvaraja, S. Massar, R. M. Osgood, Jr., P. Verheyen, J. Van Campenhout, R. Baets, W. M. J. Green, and G. Roelkens, *Nanophotonics* **5**, 1 (2016).
- [58] J. Leuthold, C. Koos, and W. Freude, *Nat. Photon.* **4**, 535 (2010).
- [59] F. D. Zong, C. Q. Dai, and J. F. Zhang, *Commun. Theor. Phys.* **45**, 721 (2006).